AnguLoc: Concurrent Angle of Arrival Estimation for Indoor Localization with UWB Radios

Milad Heydariaan
University of Houston

Hossein Dabirian
University of Houston

Omprakash Gnawali
University of Houston

Abstract—The angle of arrival (AoA) estimation is one of the commonly used techniques for indoor localization. Ultra-wideband (UWB) radios facilitate AoA estimation through the measurement of the phase difference of arrival (PDoA) at multiple receiver antennas. Concurrent transmissions in UWB radios aim to increase the efficiency of localization systems by exploiting wireless interference. This paper first investigates the feasibility of AoA estimation with UWB radios in a concurrent scheme. State-of-the-art UWB indoor localization solutions use time difference of arrival (TDoA) in a concurrent scheme. These solutions rely on accurate timestamping of the concurrently received packets. However, due to the scheduling uncertainty of the UWB transmitter platform used in this area, an unavoidable timing jitter of 8 ns causes up to 2.4 m of the localization error. Therefore, the accuracy of solutions based on concurrent TDoA relies on additional timestamp correction, which adds to the complexity of the system. Our results show that concurrent AoA estimation remains unaffected by the transmitter scheduling uncertainties. AoA-based localization techniques face two main challenges: (1) front-back ambiguity of AoA for antenna array of size two; and (2) AoA measurement device's unknown tilting. This paper then presents AnguLoc, an efficient and scalable indoor localization system that makes use of concurrent AoA estimation to reduce the number of required packet exchanges. AnguLoc uses an Angle Difference of Arrival (ADoA) technique, also generalizable to sequential AoA, to overcome the front-back angle measurement ambiguity problem, and to work with unknown tag tilting. We evaluate AnguLoc in an office environment on a recently introduced platform, Decawave PDoA node (DWM1002). Our results show that AnguLoc is 4 times faster than sequential AoA and improves the localization accuracy by up to 44.33% compared to state-of-the-art concurrency-based indoor localization solutions without relying on additional timestamp correction.

Index Terms—Ultra-wideband, UWB, Angle of Arrival, AoA, Angle Difference of Arrival, ADoA, Localization, Phase Different of Arrival, PDoA, Decawave

I. INTRODUCTION

The advancement of ultra-wideband (UWB) technologies in the past few years has facilitated accurate and precise indoor localization. Angle of arrival (AoA) estimation with UWB was introduced and demonstrated as a promising technology [6]. However, AoA-based localization is often neglected, especially for self-localization, due to two main technical challenges it raises. **Front-back ambiguity:** An array of antennas of size two cannot determine whether the arriving packet is received from the front of the antenna or the back. **AoA receiver unknown tilting:** AoA is always measured with respect to the plane of the antenna array. If the AoA receiver has an unknown tilting, the measured angle would be unknown.

The need for finding the location of people and things inside the buildings has made indoor localization an important application of the Internet of Things (IoT). The availability of low-power low-cost commercial UWB radios such as Decawave DW1000 [4] reduced the cost-related scalability challenge. Another scalability challenge emerges from wireless interference. Traditional solutions avoid or mitigate the destructive interference, which either impairs the ability to scale or decrease the efficiency of wireless systems. Concurrency in UWB-based localization systems is a recently introduced technique that aims to build scalable and efficient solutions by allowing (quasi-)simultaneous transmissions [1], [2], [8]–[10]. In this approach, the receiver utilizes the information embedded in the channel impulse response (CIR) of the concurrently received packets to estimate the time of arrival of each packet. Existing concurrency-based solutions build scalable and efficient indoor localization systems, but they often-times incur small to large errors compared to localization results in a quiet and single-transmitter setting.

The state-of-the-art UWB-based indoor concurrent localization systems, SnapLoc [8] and Chorus [2], implement a GPS-like system, where tag nodes estimate their location using time difference of arrival (TDoA) technique. Tags derive TDoA by estimating the time of arrival (ToA) for concurrently received messages from multiple anchors by analyzing the combined CIR. The accuracy of location estimates depends on the accuracy of TDoA measurements. Many of the indoor localization systems, including state of the art [2], [8], have been demonstrated on the DW1000 platform. The transmission scheduling uncertainty of DW1000 introduces a jitter of approximately 8 ns, which can cause up to 2.4 m of the localization error. The state-of-the-art solution requires the reference node to transmit additional information to tags to correct their ToA estimates. This information is either transferred to the reference node through a wired backbone or transmitted with a wireless message. The latter requires estimation of error with the knowledge of antenna delays. Both of these solutions add complexity to the system and cause scalability issues.

We explore a particular design of concurrent AoA that is unaffected by this TX scheduling uncertainty in concurrent-transmitter localization systems. Our system does not use the location of the concurrently received signal peaks for time measurement. Instead, it only relies on the phase measurement on the peaks detected using signal matching because we are

only interested in angle measurements. Thus, we avoid the need to estimate and correct for the transmitter scheduling uncertainties. To the best of our knowledge, the work described in this paper is the first demonstration of the feasibility of concurrent AoA estimation with UWB radios.

In this paper, we first explore the feasibility of concurrent AoA estimation with UWB radios. Further, we introduce AnguLoc, an efficient and scalable indoor localization system based on an angle difference of arrival (ADoA) technique to overcome the front-back angle measurement ambiguity problem and to work with the unknown tag tilting. This algorithm has no assumptions on concurrency and can also be generalized to a sequential AoA scheme. AnguLoc utilizes concurrent AoA estimation to reduce the number of required packet exchanges. AnguLoc is four times faster than sequential AoA and improves the localization accuracy by up to 44.33% compared to state-of-the-art concurrency-based indoor localization solutions without any additional timestamp correction.

In this paper, we make these contributions:

- Study the feasibility of concurrent AoA estimation with UWB radios and comparison with sequential AoA estimation baseline.
- Design, implementation, and evaluation of AnguLoc on Decawave PDoA node (DWM1002), which is slowly being released to the public and likely to become a major localization platform.

II. RELATED WORK

This study combines AoA estimation with concurrency in UWB radios and aims to build a scalable, efficient, and accurate UWB-based indoor localization system. The main research areas related to this work are described below.

A. Wireless Interference

There is a large body of work that tries to address wireless interference as an issue to avoid, prevent, or mitigate. There is some recent work that tries to leverage interference to improve some aspects of communication.

Interference Avoidance/Prevention: The devices can use random access/back-off style or TDMA style protocols to try to avoid or prevent interference. Another work shows that piggybacking UWB packets over existing network traffic reduces the traffic and avoids collisions [17]. Since carrier sensing is generally not feasible for UWB networks, IEEE 802.15.4 UWB standard [11] suggests ALOHA for channel access. Solutions similar to ALOHA are suitable for scenarios with a small number of wireless nodes, and they cannot scale because the performance drops drastically with an increase in channel utilization beyond 18% [5], [14].

Interference Mitigation: Research has shown the effectiveness of the use of non-linear filters in removing the interference [18]. Another study uses matched filters to mitigate UWB interference and correct for ranging errors [16]. Forward error correction (FEC) or retransmissions can be used to overcome packet corruption or loss in UWB. DW1000 [4]-based solutions utilize these standard techniques to work despite interference. These techniques incur large overhead and work poorly in dense or busy networks.

Interference Exploitation: Concurrent TX from multiple wireless devices is the key component of these solutions. Glossy [7] used concurrent transmissions to build a time synchronization system through network flooding while maintaining the reliability of packet reception. SurePoint [13] exploits concurrent transmissions for flooding-based time synchronization in UWB networks to increase the reliability of packet reception. Using concurrency for UWB-based localization systems was first introduced by Corbalán and Picco [1] and later improved in other studies. [2], [8]–[10]. Another study demonstrated the feasibility and performance of concurrent communication with UWB radios [22].

B. Indoor Localization

There are many indoor localization techniques developed specifically for UWB radios (Table I). Concurrency can increase the efficiency and scalability of indoor localization, but existing concurrency-based solutions fail to achieve the same level of accuracy as sequential measurement solutions.

Angle of Arrival: Many research studies explored various ways to measure AoA [12], [23], [24], including by calculating phase difference of arrival (PDoA) using two radios clocked from the same crystal oscillator [6], [15]. AoA-based localization systems typically face front-back ambiguity and AoA receiver unknown tilting problems. One way to address these two challenges is to measure AoA on the anchors' side and assume known tilting [21], [24]. Researchers developed methods to address the unknown tilting problem, but they assumed no front-back ambiguity on the angle measurements [20], [25]. Another research study uses at least 3 UWB radios on a circular shape, clocked from the same frequency oscillator, for the anchor to concurrently estimate the location of 3 tags by combining the time of flight (ToF) and phase information, but their proposed method cannot scale the number of tags [23].

Concurrent Ranging: Concurrent ranging with UWB radios was the first introduced concurrency-based localization technique [1] and there have been attempts to improve its performance [9], [10].

Concurrent Time Difference of Arrival (TDoA): Existing concurrency-based localization systems (e.g., SnapLoc [8] and Chorus [2]) use ToA information for all concurrently received packets. The main problem with *concurrent* localization systems is their failure to achieve high resolution timestamping that *sequential* localization systems can achieve which affects the quality of location estimates, i.e., 1.0016 ns for concurrent vs 15.6 ps for sequential on DW1000 platform. On the contrary, AoA estimation only relies on phase information and is not affected by timestamping jitter.

III. SYSTEM DESIGN

AnguLoc is the first system that shows how to concurrently estimate AoA. AnguLoc also provides an algorithm based on ADoA between pairs of anchors to find the location of tags.

TABLE I: UWB-based Indoor Localization Techniques

|	Localization Technique	Advantages	Disadvantages
Sequential	Two-way Ranging (TWR)	Accurate Time synchronization is not required	Not scalable High power consumption High air-utilization
	Time Difference of Arrival (TDoA)	Scalable Low power consumption for tags	Accurate time synchronization is required
	Angle of Arrival (AoA)	Low power consumption Low air-utilization Time synchronization is not required	Requires 2 UWB radios per anchor Front-back ambiguity Unknown tag tilting
Concurrent	Concurrent TWR	Saves air-time by using concurrency	Not accurate due to TX timestamping issue Not scalable
	Concurrent TDoA	Saves air-time by using concurrency	Not accurate due to TX timestamping issue Requires antenna delay calibration
	Concurrent AoA (**AnguLoc**)	Saves air-time by using concurrency Low power consumption and air-utilization Accuracy does not rely on TX timestamping	Requires 2 UWB radios per anchor
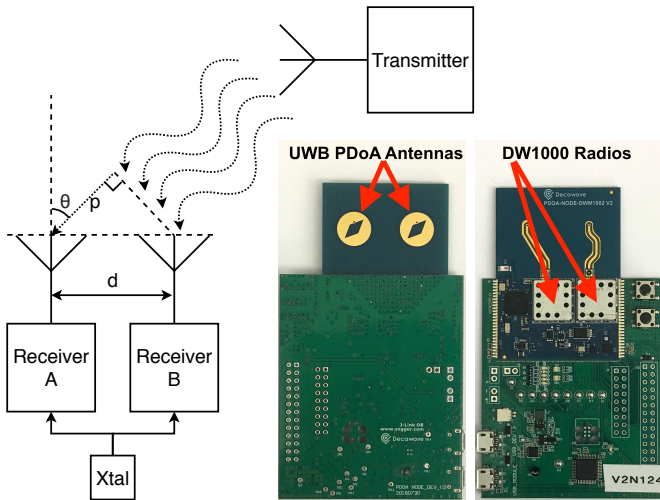
Fig. 1: Illustration of AoA, and the front and back view of the PDoA node (DWM1002). Two receivers are clocked from the same crystal oscillator (Xtal) to ensure a synchronized frequency. Arriving signals at an angle of θ cause path difference of length p which makes different PoAs at each antenna.

A. Angle of Arrival Estimation Primitives

Generally, there are four ways of performing AoA estimation using multiple UWB radios: ToF, TDoA, PDoA, and TDoA/PDoA hybrid [6]. Fig. 1 illustrates an arriving signal at an antenna array of size two. The signal travels a path difference p longer, to reach the second antenna. With an antenna separation of length d, the path difference $p = d \times \sin\theta$, where θ is defined as the angle of arrival. Time-based methods require either large antenna separation, which impacts the form factor of self-localizing tags, or extremely precise ToA estimation. Decawave DW1000 radio has a precision of 333 ps or equivalently 10 cm [4], which requires an antenna separation of at least $d = 1.14$ m for an angle of arrival precision of 5°. However, the precision

of the PDoA method depends on the carrier frequency and antenna separation. The drawback of the PDoA method is the requirement of highly precise phase synchronization between the two radios. One way to address this issue is to clock the two radios from the same frequency oscillator.

1) Mapping Phase Difference of Arrival to Angle of Arrival: We can calculate PDoA by taking the difference between individually calculated phase by each radio and mapping the PDoA to AoA. DW1000 reports CIR as a sequence of I and Q samples, representing the real and imaginary parts of each CIR sample. We can calculate the phase of arrival (PoA) of the preamble for each radio as $\arctan\frac{Q_i}{I_i}$, with i being the sample number, which DW1000 reports as the first path of the signal. Further, Decawave suggests a phase correction by deducting the start of frame delimiter (SFD) phase from the calculated PoA. Finally, PDoA (α) is the difference between corrected PoA values of each radio, mapped to $[-\pi, \pi]$. With a wavelength of λ, $p = \frac{\alpha \times \lambda}{2\pi}$. Solving for θ gives us $\theta = \arcsin\frac{\alpha\lambda}{2\pi d}$. To have a one-to-one mapping between α and θ, the antenna separation of d needs to be less than half of the wavelength ($\frac{\lambda}{2}$). Details of AoA estimation are also available in Decawave's patent [15].

2) Antenna Modification for Receiving from Front and Back: AnguLoc builds a localization system that relies on the reception of packets from all directions. The antenna designed for DWM1002 is a directional antenna that receives with a reasonable quality only from one side. To address this issue, we disconnected the antenna from DWM1002 and attached two Decawave dipole antennas. We separated the two antennas by a distance of approximately 3.75 cm, which is half the wavelength for the 4 GHz frequency channel.

3) Calibration and Correction for Antenna Characteristics: With a centimeter-level wavelength, the path difference p causes a large PDoA (α). Any asymmetry in the design of the antenna paths would cause a large difference in the phase difference at both antennas, even with an angle of 0°. For example, with the 2 cm antenna separation for 6.5 GHz
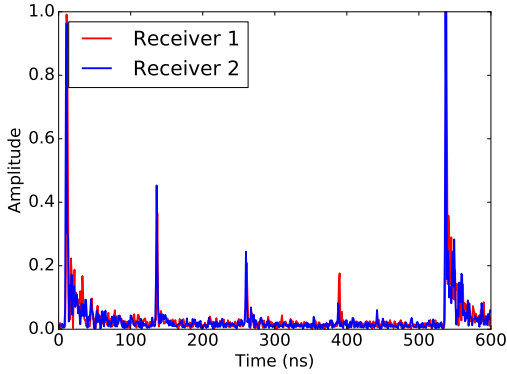
Fig. 2: CIR estimated at the PDoA node when receiving concurrently from five responders. CIR is well aligned for all responses in both receiver nodes.

Fig. 3: Concurrent transmissions protocol. First, A_{REF} broadcasts a *SYNC* packet (shown with number 1). Upon reception of *SYNC*, all anchors (A_i) broadcast a *REPLY* packet (shown with number 2). All *REPLY* packets arrive at the Tag (T) (quasi-)simultaneously.

frequency channel, 1 mm of asymmetry would translate to an error of $\arcsin \frac{0.001}{0.02} = 2.8°$. We need to calibrate each board separately for such errors by measuring the PDoA error at $0°$ and correcting the PDoA in later measurements.

With antenna separation smaller than a few wavelengths, they interact with mutual coupling, which causes the effective path difference to be different from the geometric path difference [3]. Since this behavior is non-linear, we use a polynomial correction function. By measuring at multiple samples at different angles, we fit a polynomial that corrects for the antenna characteristics. For our customized antenna, we use the following polynomial to correct the path difference p:

$$12600.13p^4 - 575.45p^3 - 12.40p^2 + 1.56p + 0 \qquad (1)$$

B. Concurrent Angle of Arrival Estimation

Concurrent AoA estimation combines the idea of AoA estimation on UWB radios with concurrent transmissions.

1) Channel Impulse Response and the Concurrency Window: CIR is obtained by accumulating cross-correlation values between the arriving stream of repeated preamble sequence and a known sequence. When preambles of multiple packets arrive at a receiver, only if they arrive in a short time window after the first packet, the correlation would be large at multiple points in CIR, showing multiple CIR peaks. We call this time window the *concurrency window*. The length of CIR is a maximum of 1016 ns, but in practice, we can use approximately half of the CIR length as the *concurrency window*. Fig. 2 shows CIR estimates for five packets arriving at two receivers in a *concurrency window*.

2) Responder Synchronization Protocol: One method to achieve concurrent transmissions and receive all responses in a *concurrency window*, is to synchronize multiple transmitters with a *SYNC* packet. As depicted in Fig. 3, all responders (anchors for localization) broadcast a *REPLY* packet when they receive the *SYNC* packet. Adding a time delay ΔR to the ToA of the *SYNC* packet helps to remove most of the system-level jitters. Finally, tags receive *REPLY* packets
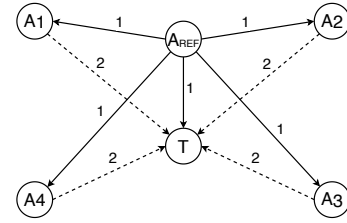
(quasi-)simultaneously. State-of-the-art concurrent localization systems [2], [8] suggest using a response position modulation. This solution resolves issues of the overlapping responses with multipath components (MPCs), and overlapping responses of the equidistant transmitters. The response position modulation is implemented by deliberately adding certain delays (δt_i) in response, in addition to the already existing response delay (ΔR). With enough delay set for δt_i, we increase the probability of peak detection since MPCs decay in further CIR samples. With the assumption of a maximum distance between transmitters, the response position modulation also helps with the problem of equidistant nodes. Similar to the state of the art, we define $\delta t_i = (i - 1) \times \alpha$, where i is the node ID, and α is set to 128 ns. Because of clock drift between responders, if we increase ΔR, the position of peak might shift in time. For $\Delta R = 25$ ms this shift goes up to 12 ns [10]. This shift in time affects the performance of response position modulation and its robustness against MPCs. We use the same time synchronization methodology used by the state of the art to avoid this problem [8], [10].

3) Detection and Extraction of Concurrent Response Peaks: Similar to concurrent localization systems, concurrent AoA estimation relies on reliable detection of concurrent responses. Without a reliable peak detection, we might misclassify noise, MPCs, and concurrent peaks. State-of-the-art concurrent localization systems [2], [8] suggest using a search and subtract (SS) algorithm to reliably find the concurrent peaks. We also adopt the SS algorithm for reliable peak detection as follows. We first extract a pulse shape for PG_DELAY of 0x95 for frequency channel 4 by transmitting packets in a noise-free environment and recording the first path of CIR and averaging them for 1000 packets. We use this pulse shape as our signal template. To detect if there is any peak from a responder and avoid detecting noise, we only consider the peak if it has an amplitude exceeding a noise threshold, $\eta = 12 \times \sigma_{\mathrm{noise}}$ [2]. The SS algorithm is as follows:

(i) Divide the CIR into multiple chunks with respect to the 128 ns delays set for each responder. The size of each window is 128 ns, centered around the position of each responder. The first window starts at 64 ns after the first peak.

(ii) Upsample each CIR chunk using FFT with the upsampling factor set to $L = 30$.

(iii) Normalize the upsampled CIR chunk.

(iv) Cross-correlate the chunk with the signal template and find the index with maximum correlation.

(v) If the sample at the found index has an amplitude exceeding a noise threshold, $\eta = 12 \times \sigma_{\text{noise}}$, we consider it as a concurrent peak.

4) Angle of Arrival Estimation for Multiple Responders: We fuse the information we extract from the CIR of the two radios to calculate AoA for each concurrent response using Algorithm 1. The inputs of the algorithm are the maximum number of concurrent responses expected, CIR from the first radio, and CIR from the second radio. $FindPeaks$ is the function that extracts concurrent peaks using the method described in Sec. III-B3. $Peaks$ is a 2D array containing the time sample index indicating the presence of each peak. Finally, we feed the found peak pairs from both radios belonging to each concurrent response to $CalcAoA$, the AoA calculation function described in Sec. III-A1, to calculate and output the concurrent AoA estimates.

Algorithm 1 Concurrent AoA Estimation

Input: $MaxNumResponses, CIR_1[], CIR_2[]$
Output: $AoA[]$
  $N \leftarrow MaxNumResponses$
  $Peaks[1 \ldots N][1] \leftarrow FindPeaks(N, CIR_1[])$
  $Peaks[1 \ldots N][2] \leftarrow FindPeaks(N, CIR_2[])$
  for $i \leftarrow 1$ to N **do**
    $AoA[i] \leftarrow CalcAoA(Peaks[i][1, 2], CIR_1[], CIR_2[])$
  end for

C. Concurrent AoA vs. Concurrent TDoA

We compare concurrent AoA estimation systems with concurrent TDoA systems to understand concurrent AoA (what we propose) with respect to concurrent TDoA (which has been discussed in the literature).

1) Fusing Information from Multiple Radios: For AoA estimation, we need a receiver with multiple radios to measure the phase on different antennas and combine them to estimate AoA. Doing such measurements requires that the radios are synchronized in phase. Clocking radios from the same crystal oscillator helps synchronize the phase, but it also requires careful design of the hardware. To ensure phase synchronization, we need to minimize any asymmetry in the board in both antenna path and clock path. For TDoA estimation, we need a receiver with one radio, which makes the design of the hardware simpler.

2) Working with Phase instead of Time: For AoA estimation, we need to work with phase information rather than time information, which is used by TDoA estimation. The main advantage of working with phase information is the immunity against time scheduling uncertainties and jitters in the transmitters. TDoA systems rely on the difference in ToA for packets from multiple transmitters. Concurrent TDoA systems rely on synchronized transmissions. Hence, any jitter or scheduling uncertainties affect their performance negatively. The jitters do not impact concurrent AoA estimation systems at the transmitters since we only work with the PDoA at the receiver for each transmitter. Hence, concurrent AoA systems are immune to timing jitters.

D. Angular Localization Algorithm

AnguLoc uses angle differences between pairs of anchors for localization and is considered as an ADoA algorithm. AnguLoc extends the ADoA algorithm [25] to address the front-back ambiguity issue. We assume nothing about the concurrency; hence, our algorithm is also generalizable to sequential AoA. We assume N anchors positioned at $A_i = (x_i, y_i)$ ($1 \leq i \leq N$), and a tag having unknown angle θ and position $T = (x, y)$. In the case of known tag tilting, at least three anchors are required to find the tag position, since there are only two angle differences for three anchors and we have two unknowns (x, y). For the case of unknown tag tilting, we need $N \geq 4$. Suppose the line segment connecting i^{th} and j^{th} anchors subtends angle difference $\theta_{i,j}$ from the tag. Regarding tag and these two anchors, there are two different possibilities, as illustrated in Fig. 4. The first possibility is that the *tag antenna plane* and the passing line segment intersect. The second possibility is that they do not intersect. In the first case, $\theta_{i,j} = \theta_1 + \theta_2$ and in the second case $\theta_{i,j} = |\theta_1 - \theta_2|$. Since we have front-back ambiguity for angle measurements, we cannot identify which case is correct if we do not know the tag tilting. But, with the assumption that we know which scenario happens for all pairs of anchors, $\theta_{i,j}$ values are known up to a white Gaussian noise. We denote these measured noisy angles $\hat{\theta}_{i,j}$. On the other hand, the exact angles must be:

$$\theta_{i,j} = \arccos(\frac{TA_i \cdot TA_j}{|TA_i||TA_j|}) =$$
$$\arccos(\frac{(x - x_i)(x - x_j) + (y - y_i)(y - y_j)}{\sqrt{((x - x_i)^2 + (y - y_i)^2)((x - x_j)^2 + (y - y_j)^2)}})$$
$$(2)$$

where TA_i and TA_j are vectors from tag to anchors i and j, and $\cdot$ is the inner product operation. Therefore, one can define the following least square cost function:

$$J(x, y) = \sum_{j > i} (\theta_{i,j} - \hat{\theta}_{i,j})^2 \qquad (3)$$

Finally, the position can be estimated as:

$$\hat{T} = \underset{x,y}{\text{argmin}} \, J(x, y) \qquad (4)$$

As illustrated in Fig. 5 with four anchors, there are only six possible cases for *tag antenna plane*, depending on the tag tilting. First, AnguLoc finds the optimum solution $\hat{T}(x, y)$ for Eq. 4 for all six different cases. Then, AnguLoc chooses the solution where the residual value of $J(x, y)$ is minimum among the six cases. To find each $\hat{T}(x, y)$, we use the quasi-Newton method [19] with an initial position estimate at the center of the room. To see the typical performance of

the algorithm, we use simulation. We chose 10 random tag locations in a 5 m × 5 m room with four anchors placed in the corners. For each tag location, we chose 20 random tag tilting uniformly spread over the interval of $[0°, 360°]$. For each tag location and tilting, we repeated the simulation 10 times and added random noise each time to the angle measurements. For each resulting simulated noisy measurement, we run the ADoA-based algorithm and record the residual error as the Euclidean distance between the ground truth and estimated location. Fig. 6 shows the CDF of error for different standard deviations of noise from 2.5° to 10°. For noise levels below 5°, we can say that the algorithm has a sub-meter error 80% of the time.
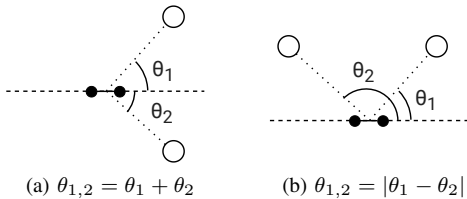

(a) $\theta_{1,2} = \theta_1 + \theta_2$ (b) $\theta_{1,2} = |\theta_1 - \theta_2|$

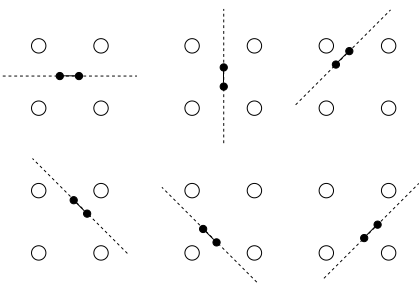Fig. 4: Angle difference and *tag antenna plane*

Fig. 5: Angle difference in six different cases for four-anchor setting.
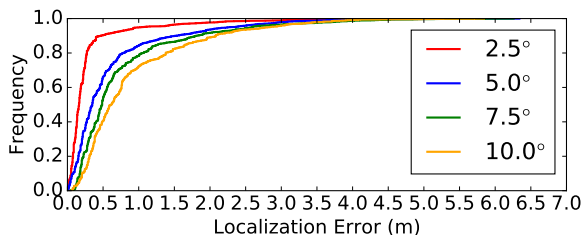

Fig. 6: Typical performance of our ADoA algorithm simulated for different levels of angle measurement noise. The localization error is below 1 m in 80% of the time for noise levels below 5°.

IV. EVALUATION

A. Experimental Setup

In our experiments, we used Decawave PDoA Node DWM1002 (Fig. 1) as our tag, with the modified antennas to receive from both sides. For responders/anchors, we used
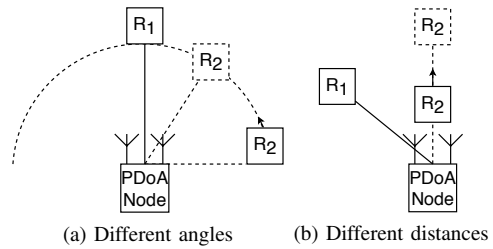

(a) Different angles   (b) Different distances

Fig. 7: Experimental setup

TABLE II: AoA Estimation Baseline Performance

(a) Angles

θ (°)	AoA Error (°)			
	Avg	Std	50th	90th
-90	0.63	2.60	0.00	0.00
-60	4.56	3.38	3.86	8.69
-30	2.42	1.81	2.07	4.82
0	3.24	2.21	2.73	6.52
30	3.20	2.46	2.59	6.44
60	4.89	3.31	4.19	9.52
90	0.51	2.77	0.00	0.00

(b) Distances

d (m)	AoA Error (°)			
	Avg	Std	50th	90th
3	2.12	1.63	1.65	4.51
6	2.29	1.72	1.92	4.73
9	2.52	1.85	2.26	5.01
12	2.41	1.75	2.01	4.90
15	3.30	2.49	2.83	6.24

the radinoL4 DW1000 platform. We set up our system in an academic building in a hallway of size 20 m × 3 m for concurrent AoA evaluation experiments and inside a room of size 6.5 m × 4.5 m for localization experiments. In all experiments, we placed all the nodes on tripods on 1.5 m height. We used frequency channel 4, with a preamble length of 64, a pulse repetition frequency (PRF) of 64 MHz, and a data rate of 6.8 Mbps.

B. Feasibility of Concurrent AoA

We placed the DWM1002 node in a fixed position and measured the AoA in different angles by placing the responder nodes in various angles and distances, as illustrated in Fig. 7. The ground truth angle, θ, is the angle between the transmitter and center of the receiver antennas.

1) Platform AoA Estimation Baseline: We use a single-responder setting with DWM1002 in AoA estimation for different angles and distances as the baseline. Our work is the first paper to show the performance of DWM1002. Table II shows the baseline AoA estimation performance. AoA estimation has an error of less than 10° in 90% of the time for all angles. The antenna path correction polynomial (discussed in Sec. III-A3) compresses all the measurements near the antenna edges to 90° and -90°, and we get almost 0° error in 90% of the time. However, if the transmitter is not facing the receiver at the antenna edges, we get higher errors. For the distance increment experiment (Fig. 7b), we placed the responder node at 20° and increased its distance. Table IIb shows that the AoA error increase by increasing the distance because of the negative effects of path loss on performance.

2) Concurrent AoA in Different Angles: To evaluate concurrent AoA estimation, we fix R_1 at 0° and rotate R_2 (Fig. 7a) and measure angles for both nodes concurrently.

TABLE III: Concurrent AoA Performance – Angles

θ_2 (°)	R_1 AoA Error (°)				R_2 AoA Error (°)			
	Avg	Std	50th	90th	Avg	Std	50th	90th
-90	3.29	2.37	2.74	5.97	0.40	2.07	0.00	0.00
-60	3.39	2.38	3.06	6.53	6.68	4.40	6.26	12.52
-30	4.23	2.66	4.09	7.53	3.76	3.20	2.51	8.73
0	5.10	2.56	5.34	8.25	5.18	2.46	5.22	8.54
30	4.03	2.76	3.77	7.48	4.56	3.90	3.29	10.29
60	4.01	2.44	3.99	7.41	5.53	4.17	5.02	11.71
90	3.23	5.24	2.32	6.15	1.00	3.45	0.00	1.68

TABLE IV: Concurrent AoA Performance – Distances

d_2 (m)	R_1 AoA Error (°)				R_2 AoA Error (°)			
	Avg	Std	50th	90th	Avg	Std	50th	90th
3	3.15	2.12	2.90	5.75	2.86	2.15	2.32	5.86
6	2.61	1.64	2.44	5.15	3.61	3.40	2.57	8.41
9	2.71	1.73	2.42	4.82	3.09	2.53	2.42	6.17
12	2.72	2.07	2.27	5.48	5.17	4.02	4.24	11.84
15	2.76	2.04	2.65	5.55	8.37	4.57	9.21	14.12

Fig. 8a compares the ground truth angle with the estimated AoA for R_2 concurrently, while showing the results of baseline AoA experiments. Table III compares the performance of concurrent AoA for both R_1 and R_2. Results are comparable with baseline AoA estimation performance. We also switched R_1 and R_2 and observed similar results. 0° errors are due to compression of measurements near the antenna edges to -90° and 90° by path correction polynomial. We can conclude that the concurrency does not significantly affect the AoA estimation.

(a) Concurrent AoA in different angles.
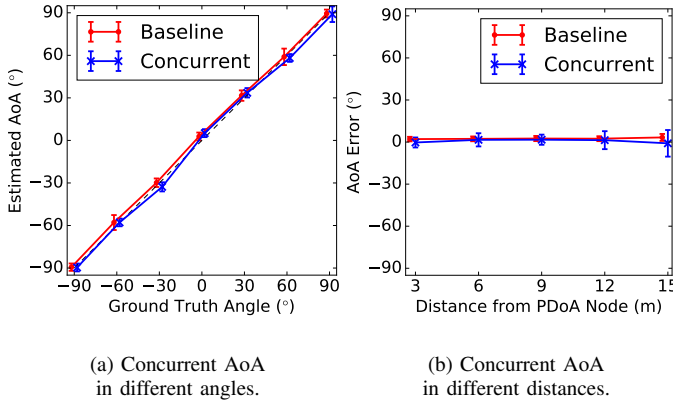
(b) Concurrent AoA in different distances.

Fig. 8: Evaluation of concurrent AoA estimation. Concurrency does not impact the quality of AoA estimation. Each point represents the mean value for 100 measurements and error bars are one standard deviation.

3) Concurrent AoA in Different Distances: We fix R_1 at 30° and move R_2 away at 0° (Fig. 7b) and measure angles for both nodes concurrently. Fig. 8b compares the concurrent AoA error in different distances for R_2 while showing the results of baseline AoA experiments. At distances beyond 12 m, the path loss for the farther node decreases the performance, since the concurrent peak size shrinks. Table IV compares the performance of concurrent AoA for both R_1 and R_2. Results are comparable with baseline AoA estimation performance. We also switched R_1 and R_2 and observed similar results. In this case, at longer distances of R_1, the path loss for R_1 is much higher than R_2, causing failure to receive the packet from R_1. We can conclude that the concurrency does not significantly affect the AoA estimation in small distances.
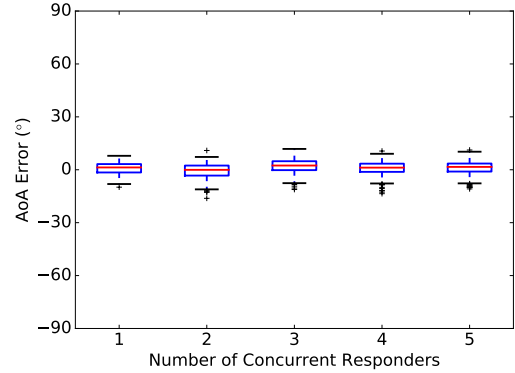

Fig. 9: AoA error does not increase with the increase in number of concurrent responders in the network. Each box plot represents combined errors from all nodes present in the network for 100 measurements.

4) Scaling the System Beyond Two Responders: We investigate how adding more responders affect the quality of AoA estimation for each responder. For this purpose, we added more responders to the network over time. Fig. 9 shows the AoA error, combined from concurrent AoA measurements from all responders present in the network. We observe that the error does not increase by adding more responders up to 5 nodes. When we add more responders to the network, we cannot receive most of the packets from the first responder. When a concurrent peak is more than half a preamble symbol away from the first responder, it is hard for the receiver to distinguish which of the responders' signals arrived first. In this case, we receive the packet from the last responder instead.

C. Indoor Localization with AnguLoc

We placed four anchors in the corners of a room, more specifically at (0 m, 0 m), (3 m, 0 m), (0 m, 6 m), and (3 m, 6 m). To see the performance of AnguLoc, we first placed our tag node at 10 different locations in the room, at angles of 0°, 45°, and 90°. For each setting, we collected more than 100 data points, resulting in a total of 3000 location estimates. Second, we collected data for a mobile tag moving in the room on a rectangular shape path, 50 cm away from the borders. We moved the tag at a constant speed to make it easier to approximate the ground truth. For the mobile setting, we collected more than 200 data points. We run AnguLoc on the collected data, as well as state-of-the-art concurrent TDoA algorithm for comparison. We did

not implement timestamp correction methods suggested by SnapLoc [8]. Fig. 10 shows the CDF of localization error for both static and mobile experiments, comparing AnguLoc and concurrent TDoA (CTDoA) method. In the static setting, the 90th percentile of error for AnguLoc is 0.67 m, and for CTDoA is 1.20 m. In the mobile setting, the 90th percentile of error for AnguLoc is 1.11 m, while it is 1.41 m for CTDoA. AnguLoc improves the localization accuracy by 44.33% in the static setting and by 21.46% in the mobile setting, compared to the CTDoA method without timestamp correction. AnguLoc takes more time than CTDoA to estimate the location since it has to solve six optimization problems to consider every tag tilting possibilities.
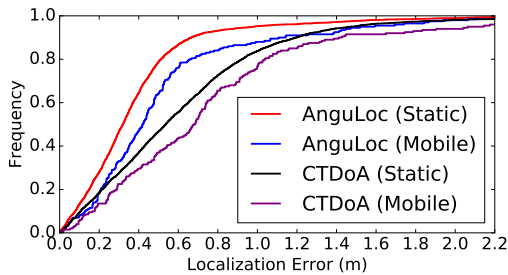

Fig. 10: CDF of localization error for AnguLoc and concurrent TDoA, with static and mobile tag. AnguLoc outperforms concurrent TDoA method. CDF for static tags is aggregated for more than 3000 location estimates. CDF for mobile tags is aggregated for more than 200 location estimates.

V. DISCUSSION

Scaling Concurrent Transmissions: Current concurrent transmission systems do not scale beyond a handful of anchors. In the case of more radio nodes, we can make multiple groups of concurrent nodes. We can assign a timeslot to each group. All nodes in one group respond (quasi-)simultaneously in the timeslot assigned to their group.

Angle of Arrival Estimation: (1) The weaker reception on the sides of dipole antennas causes a larger AoA error. (2) With the increase in distance, the performance of concurrent AoA decreases due to lower SNR. One solution is to increase the density of anchors and select the nearest anchors for localization.

VI. CONCLUSIONS

AnguLoc is the first concurrent AoA system on UWB radios. We showed that concurrent AoA can be used with a small yet sufficient number of concurrent transmitters without performance degradation compared to sequential AoA. AnguLoc enables efficient, accurate, and scalable indoor localization. Our ADoA-based localization algorithm overcomes the front-back angle measurement ambiguity problem, which uncovers the neglected capabilities of AoA-based localization. Facilitating self-localization in AoA-based systems increases scalability to an unlimited number of tags. Further, equipping such systems with concurrent AoA measurement capability increases the efficiency without loss of accuracy. AnguLoc is four times faster than sequential AoA when using four anchors while maintaining a sub-meter accuracy and supporting an unlimited number of tags.

REFERENCES

[1] P. Corbalán and G. P. Picco. Concurrent ranging in ultra-wideband radios: Experimental evidence, challenges, and opportunities. In *EWSN*, 2018.

[2] P. Corbalán, G. P. Picco, and S. Palipana. Chorus: UWB concurrent transmissions for GPS-like passive localization of countless targets. In *IPSN*, 2019.

[3] Decawave. *PDOA Primer - Calculating position directly from range and phase difference of arrival at two antennas*, 2018.

[4] Decawave. *DW1000 Datasheet*, 2020.

[5] Decawave. *DW1000 User Manual*, 2020.

[6] I. Dotlic, A. Connell, H. Ma, J. Clancy, and M. McLaughlin. Angle of arrival estimation using Decawave DW1000 integrated circuits. In *WPNC*. IEEE, 2017.

[7] F. Ferrari, M. Zimmerling, L. Thiele, and O. Saukh. Efficient network flooding and time synchronization with glossy. In *IPSN*. IEEE, 2011.

[8] B. Groβwindhager, M. Stocker, M. Rath, C. A. Boano, and K. Römer. Snaploc: an ultra-fast UWB-based indoor localization system for an unlimited number of tags. In *IPSN*, 2019.

[9] B. Großwindhager, C. A. Boano, M. Rath, and K. Römer. Concurrent ranging with ultra-wideband radios: From experimental evidence to a practical solution. In *ICDCS*. IEEE, 2018.

[10] M. Heydariaan, H. Mohammadmoradi, and O. Gnawali. R3: Reflection resilient concurrent ranging with ultra-wideband radios. In *DCOSS*. IEEE, 2019.

[11] IEEE. IEEE std 802.15.4-2011, IEEE standard for local and metropolitan area networks—part 15.4: Low-rate wireless personal area networks (LR-WPANs), 2011.

[12] C. R. Karanam, B. Korany, and Y. Mostofi. Magnitude-based angle-of-arrival estimation, localization, and target tracking. In *IPSN*, 2018.

[13] B. Kempke, P. Pannuto, B. Campbell, and P. Dutta. SurePoint: Exploiting ultra wideband flooding and diversity to provide robust, scalable, high-fidelity indoor localization. In *SenSys*. ACM, 2016.

[14] C. Li, H.-B. Li, and R. Kohno. Performance evaluation of IEEE 802.15.4 for wireless body area network (WBAN). In *ICC*. IEEE, 2009.

[15] M. McLaughlin, D. Neirynck, and C. McElroy. Timing recovery for use in an ultra-wideband communication system, May 17 2018. US Patent App. 15/868,026.

[16] H. Mohammadmoradi and O. Gnawali. Study and mitigation of non-cooperative UWB interference on ranging. In *EWSN*, 2019.

[17] H. Mohammadmoradi, M. Heydariaan, and O. Gnawali. SRAC: Simultaneous ranging and communication in UWB networks. In *DCOSS*. IEEE, 2019.

[18] D. K. Rout and S. Das. Multiple narrowband interference mitigation using hybrid hermite pulses for body surface to external communications in uwb body area networks. *Wireless Networks*, 2017.

[19] D. F. Shanno. Conditioning of quasi-newton methods for function minimization. *Mathematics of computation*, 1970.

[20] H.-J. Shao, X.-P. Zhang, and Z. Wang. Efficient closed-form algorithms for AOA based self-localization of sensor nodes using auxiliary variables. *Signal Processing*, 2014.

[21] Z. Tian, Y. Li, M. Zhou, and Y. Lian. WLAN indoor localization using angle of arrival. In *MLICOM*. Springer, 2017.

[22] D. Vecchia, P. Corbalán, T. Istomin, and G. P. Picco. Playing with fire: Exploring concurrent transmissions in ultra-wideband radios. In *SECON*, 2019.

[23] T. Wang, H. Zhao, and Y. Shen. An efficient single-anchor localization method using ultra-wide bandwidth systems. *Applied Sciences*, 2020.

[24] S. Wielandt and L. D. Strycker. Indoor multipath assisted angle of arrival localization. *Sensors*, 2017.

[25] B. Zhu, J. Cheng, Y. Wang, J. Yan, and J. Wang. Three-dimensional VLC positioning based on angle difference of arrival with arbitrary tilting angle of receiver. *JSAC*, 2017.